

# Practical and Bilateral Privacy-preserving Federated Learning

Yan Feng<sup>1 2 \*</sup> Xue Yang<sup>1 2 \*</sup> Weijun Fang<sup>1 2 \*</sup> Shu-Tao Xia<sup>1 2</sup> Xiaohu Tang<sup>3</sup>

## Abstract

Federated learning, as an emerging distributed training model of neural networks without collecting raw data, has attracted widespread attention. However, almost all existing researches of federated learning only consider protecting the privacy of clients, but not preventing model iterates and final model parameters from leaking to untrusted clients and external attackers. In this paper, we present the first bilateral privacy-preserving federated learning scheme, which protects not only the raw training data of clients, but also model iterates during the training phase as well as final model parameters. Specifically, we present an efficient privacy-preserving technique to mask or encrypt the global model, which not only allows clients to train over the noisy global model, but also ensures only the server can obtain the exact updated model. Detailed security analysis shows that clients can access neither model iterates nor the final global model; meanwhile, the server cannot obtain raw training data of clients from additional information used for recovering the exact updated model. Finally, extensive experiments demonstrate the proposed scheme has comparable model accuracy with traditional federated learning without bringing much extra communication overhead.

## 1. Introduction

With the continued emergence of privacy breaches and data abuse (Wikipedia, 2018), data privacy and security issues gradually impede the flourishing development of deep learning (Yang et al., 2019). In order to solve the privacy concerns of users, *federated learning* (FL) (McMahan et al., 2017) has recently been presented as a promising solution, where many clients collaboratively train a shared global model under the orchestration of a central server, while ensuring that

each client’s raw data is stored locally and not exchanged or transferred. Based on the type of clients, FL is divided into two settings (Kairouz et al., 2019): the cross-device FL, where clients are mobile or edge devices, and the cross-silo FL, where clients are relatively reliable organizations (e.g., medical or financial institutions). In this paper, we focus on solving the challenges faced in the cross-silo FL that has received greatly interests recently.

Recently, many FL algorithms (McMahan et al., 2017; Bonawitz et al., 2017) and the corresponding variants (Li et al., 2019c;b) have been developed to show its potential value in applications such as healthcare (Li et al., 2019b) and vehicle-to-vehicle communication (Samarakoon et al., 2018). Almost all existing researches focus on protecting local training data from disclosing through uploaded gradients, however, not consider protecting the intermediate iterates and the final model parameters from disclosing. In fact, for the cross-silo FL, clients (e.g., medical or financial institutions) contribute their data and consume resources (e.g., computation and communication) to collaboratively train a shared global model to gain wealth (Liu et al., 2016). Thus, it is necessary to protect the global model from disclosing to external entities. In addition, due to competition among clients, it is impossible to ensure that all clients are trusted and not curious about the training data of others. In other words, they may try to obtain some additional information from the intermediate iterates during the training or final model parameters. Therefore, it is meaningful and urgent to design a solution of FL that can further protect the intermediate iterates and the final model parameters.

Although some existing privacy-preserving techniques, like differential privacy (Dwork et al., 2006) and homomorphic encryption (Phong et al., 2018), seem to be alternatives, they cannot address the above problem well. For example, the differential privacy technique usually involves a trade-off between accuracy and privacy, and cannot maintain the sparsity of the model updates (Kairouz et al., 2019). The homomorphic encryption is achieved at the expense of high computational and communication overhead. Furthermore, as described in (Yang et al., 2019), existing homomorphic encryption can only deal with the bounded polynomial operations, but cannot effectively address the non-linear activation functions used in deep learning.

\*Equal contribution <sup>1</sup>Tsinghua University <sup>2</sup>Peng Cheng Laboratory <sup>3</sup>Southwest Jiaotong University. Correspondence to: Xue Yang <xueyang.swjtu@gmail.com>.

As stated in (Kairouz et al., 2019), it is still a big challenge to further effectively protect intermediate iterates and final model parameters on the traditional FL. In this paper, we present a first *Practical and Bilateral Privacy-preserving Federated Learning* (PBPFL) scheme, where the main contributions are three-fold:

(1) We present a new privacy-preserving technique to encrypt intermediate iterates and final model parameters, which allows clients to train model updates on noisy intermediate iterates. The technique is versatile and applicable to most state-of-the-art models. More importantly, it ensures that only the server can obtain accurate model updates.

(2) Security analysis demonstrates that under the privacy-preservation of the traditional FL, any honest-but-curious client cannot get intermediate iterates and local training data of others during the training, even in collusion with some clients. After completing the training, clients can only use the final model (i.e., obtain the correct prediction), but cannot know model parameters.

(3) Extensive experiments conducted on real-world data demonstrate the effectiveness of our scheme compared with the traditional FL, and the efficiency of computation and communication.

## 2. Preliminaries and Problem Statement

In this section, we first outline the concept of cross-silo FL and the Hadamard product. After that, we state the system model, threat model and design goals.

### 2.1. The Cross-Silo FL

In the cross-silo FL (Kairouz et al., 2019), clients are different organizations (e.g. medical or financial), the network connection is relatively stable and the network bandwidth is relatively large. That is, all clients are always available and can afford relatively large communication cost. Thus, the cross-silo FL allows all clients to join each iteration.

Formally, consider the FL with  $K$  clients, where the  $k$ -th client has the local training dataset  $\mathcal{D}_k = \{(\mathbf{x}_i, \bar{\mathbf{y}}_i)\}_{i=1}^{N_k}$ , where  $\mathbf{x}_i = (x_{i1}, \dots, x_{id})^T$  and  $\bar{\mathbf{y}}_i = (\bar{y}_{i1}, \dots, \bar{y}_{ic})^T$  are the feature vector and the ground-truth label vector, respectively. Thus, the cross-silo FL aims to solving an optimization problem (McMahan et al., 2017; Li et al., 2019c):

$$\min_W F(W) \triangleq \sum_{k=1}^K \frac{N_k}{N} F_k(W), \quad (1)$$

where  $N$  is the total sample size such that  $N = \sum_{k=1}^K N_k$ , and  $F_k(W)$  is the local object of the  $k$ -th client such that

$$F_k(W) \triangleq \frac{1}{N_k} \sum_{i=1}^{N_k} \mathcal{L}(W; (\mathbf{x}_i, \bar{\mathbf{y}}_i)), \quad (2)$$

where  $\mathcal{L}(\cdot; \cdot)$  is the specific loss function. In this paper, we adopt the mean square error (MSE) loss function

$$\mathcal{L}(W; (\mathbf{x}_i, \bar{\mathbf{y}}_i)) = \frac{1}{2} \|\mathbf{y}_i - \bar{\mathbf{y}}_i\|_2^2, \quad (3)$$

where  $\|\cdot\|_2$  is  $l_2$  norm of a vector, and  $\mathbf{y}_i$  is the prediction.

In general, this optimization problem can be handled with stochastic gradient descent (SGD). Thus, each client first computes local gradients by adopting the SGD technique and returns them to the server for aggregation and updating

$$W_{t+1} \leftarrow W_t - \eta \sum_{k=1}^K \frac{N_k}{N} \nabla F_k(W_t), \quad (4)$$

where  $\nabla F_k(W_t)$  is the local gradient on local data of  $k$ -th client at the current model  $W_t$ , and  $\eta$  is the learning rate.

### 2.2. Hadamard Product

The Hadamard product (Horn & Johnson, 2012) takes two matrices of the same dimensions and produces another matrix of the same dimension as the operands.

**Definition 1.** For two matrices  $A$  and  $B$  of the same dimension  $m \times n$ , the Hadamard product  $A \circ B$  is a matrix of the same dimension as the operands, with elements given by  $(A \circ B)_{ij} = A_{ij}B_{ij}$ .

Besides, two properties of Hadamard product used in our scheme are given as follows:

(1) For any two matrices  $A$  and  $B$ , and a diagonal matrix  $D$ , we have

$$D(A \circ B) = (DA) \circ B \text{ and } (A \circ B)D = (AD) \circ B$$

(2) For any two vectors  $\mathbf{a}$  and  $\mathbf{b}$ , we have  $\mathbf{a} \circ \mathbf{b} = D_{\mathbf{a}}\mathbf{b}$ , where  $D_{\mathbf{a}}$  is the corresponding diagonal matrix with the vector  $\mathbf{a}$  as its main diagonal.

### 2.3. Problem Statement

In this part, we introduce the system and threat models considered in this paper, and identify our design goals.

#### 2.3.1. SYSTEM MODEL

As shown in Fig. 1, our system model mainly includes two components: a server and a number of clients, where the corresponding roles are described as follows:

**The server** is responsible for initializing the model and assisting clients in training the global model. Particularly, in order to protect the privacy, the server sends the noisy models to clients for training.

**Clients** have their own local training data and want to collaboratively train a global model. Specifically, each client

computes local gradients with their own data and the noisy model received from the server, and then returns noisy local gradients to the server for aggregating and updating.

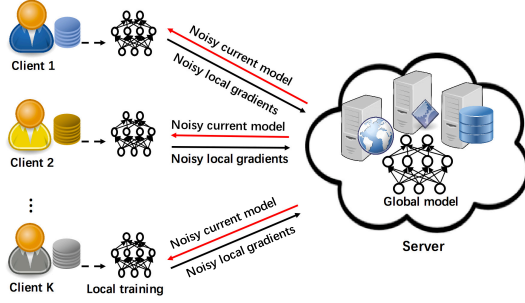


Figure 1. System architecture of the proposed scheme.

### 2.3.2. THREAT MODEL AND DESIGN GOALS

Similar to (Kairouz et al., 2019), we assume the server and clients are honest-but-curious (Hitaj et al., 2017; Phong et al., 2018), which means that they honestly follow the underlying scheme, but attempt to infer other entities' data privacy independently. Particularly, we allow each client to collude with multiple clients to get the most offensive capabilities. Besides, an eavesdropper is also considered here, who tries to obtain information from the observed data obtained by eavesdropping.

From the above, the design goals of our PBPFL mainly include the following three aspects:

**(1) Functionality:** Each client can only train models over noisy intermediate iterates, meanwhile, only the server can recover the exact model updates during the training phase and the true final model parameters during interface phase.

**(2) Privacy-preservation:** Clients know neither local training data of others nor intermediate iterates and the final model parameters. Meanwhile, the server cannot obtain the training data of clients from the received information.

**(3) Efficiency:** The proposed scheme should minimize extra computation and communication overhead without reducing model accuracy.

## 3. Proposed Scheme

In this section, we introduce our PBPFL scheme, which mainly includes four parts: parameter perturbation (server-side), noisy gradient computation (client-side), model update (server-side), and data processing (server-side).

### 3.1. Parameter Perturbation

The parameter perturbation is performed by the server, which takes model parameters  $W$  and random noises  $R$

as inputs, and outputs noisy model parameters  $\widehat{W}$ <sup>1</sup>. In order to facilitate the understanding of our encryption method, we give a simple case of multiple layer perceptron (MLP) with ReLU non-linear activation. Then, we show this method can be easily applied on the state-of-the-art models such as ResNet(He et al., 2016) and DenseNet(Huang et al., 2017).

#### 3.1.1. MULTIPLE LAYER PERCEPTRON

Consider a MLP with  $L$  layers, where the parameter and the output of the  $l$ -th layer are denoted as  $W^{(l)} \in \mathbb{R}^{n_l \times n_{l-1}}$  and  $y^{(l)} \in \mathbb{R}^{n_l}$ , respectively, and  $n_l$  is the number of neurons in the  $l$ -th layer. Specifically,  $y^{(l)}$  is computed as

$$y^{(l)} = \begin{cases} \text{ReLU}(W^{(l)} y^{(l-1)}), & \text{for } 1 \leq l \leq L-1. \\ W^{(L)} y^{(L-1)}, & \text{for } l = L. \end{cases} \quad (5)$$

Note that when  $l = 1$ , then  $y^{(0)}$  is the input of neural network  $x = (x_1, x_2, \dots, x_d)^T$ .

**1. Parameter encryption.** In order to encrypt the model parameter  $W = \{W^{(l)}\}_{l=1}^L$ , the server first randomly selects the multiplicative noisy vector  $r^{(l)} \in \mathbb{R}_{>0}^{n_l}$  for  $1 \leq l \leq L-1$ , the additive noisy vector  $r_a \in \mathbb{R}^{n_L}$  with pairwise different components, and a random coefficient  $\gamma \in \mathbb{R}$ . Then, the server computes

$$\widehat{W}^{(l)} = \begin{cases} R^{(l)} \circ W^{(l)}, & \text{for } 1 \leq l \leq L-1, \\ R^{(L)} \circ W^{(L)} + R^a, & \text{for } l = L, \end{cases} \quad (6)$$

where  $R^{(l)} \in \mathbb{R}^{n_l \times n_{l-1}}$  and  $R^a \in \mathbb{R}^{n_L \times n_{L-1}}$  satisfy

$$R_{ij}^{(l)} = \begin{cases} r_i^{(1)}, & \text{when } l = 1 \\ r_i^{(l)} / r_j^{(l-1)}, & \text{when } 2 \leq l \leq L-1 \\ 1 / r_j^{(L-1)}, & \text{when } l = L \end{cases} \quad (7)$$

$$R_{ij}^a = \gamma \cdot r_{a,i} \quad (8)$$

where the subscripts  $i$  and  $j$  in Eq. (7), satisfy that  $i \in [1, n_l]$  and  $j \in [1, n_{l-1}]$ , and in Eq. (8),  $i \in [1, n_L]$  and  $j \in [1, n_{L-1}]$ .

Finally, the server sends  $\widehat{W} = \{\widehat{W}^{(l)}\}_{l=1}^L$  together with  $r_a$  to each client for local training.

**2. Forward propagation.** In order to facilitate the understanding of our parameter perturbation method, we introduce the forward propagation in advance. According to Eq. (5), each client computes the noisy output  $\hat{y} = \{\hat{y}^{(l)}\}_{l=1}^L$  with the received  $\widehat{W}$  and the sample  $(x, y)$ , i.e.,

$$\hat{y}^{(l)} = \begin{cases} \text{ReLU}(\widehat{W}^{(l)} \hat{y}^{(l-1)}), & \text{for } 1 \leq l \leq L-1. \\ \widehat{W}^{(L)} \hat{y}^{(L-1)}, & \text{for } l = L. \end{cases} \quad (9)$$

<sup>1</sup> In the rest of the paper, the notations with the symbol “ $\widehat{\cdot}$ ” indicate the parameters that are affected by the noise, e.g.,  $\widehat{W}$ ,  $\hat{y}^{(l)}$ .

In the following lemma, we present the important relations between the noisy outputs and the true outputs.

**Lemma 1.** *For any  $1 \leq l \leq L$ , the noisy output vector  $\hat{\mathbf{y}}^{(l)}$  and the true output vector  $\mathbf{y}^{(l)}$  have the following relationships*

$$\hat{\mathbf{y}}^{(l)} = \mathbf{r}^{(l)} \circ \mathbf{y}^{(l)}, \quad \text{when } 1 \leq l \leq L-1. \quad (10)$$

$$\hat{\mathbf{y}}^{(L)} = \mathbf{y}^{(L)} + \gamma \alpha \mathbf{r}_a = \mathbf{y}^{(L)} + \alpha \mathbf{r}, \quad \text{when } l = L. \quad (11)$$

where  $\alpha = \sum_{j=1}^{n_{L-1}} \hat{\mathbf{y}}_j^{(L-1)}$  and  $\mathbf{r} = \gamma \mathbf{r}_a$ .

*Proof.* Based on Eq. (7), we can deduce that  $R^{(1)} = D_{\mathbf{r}^{(1)}} E^{(1)}$ ,  $R^{(l)} D_{\mathbf{r}^{(l-1)}} = D_{\mathbf{r}^{(l)}} E^{(l)}$  for  $1 \leq l \leq L-1$ , and  $R^{(L)} D_{\mathbf{r}^{(L-1)}} = E^{(L)}$ , where  $E^{(l)}$  is the  $n_l \times n_{l-1}$  matrix whose entries are all 1s.

First, we prove Eq. (10) by induction. When  $l = 1$ , we can obtain that

$$\begin{aligned} \hat{\mathbf{y}}^{(1)} &= \text{ReLU}(\widehat{W}^{(1)} \mathbf{x}) = \text{ReLU}((R^{(1)} \circ W^{(1)}) \mathbf{x}) \\ &= \text{ReLU}((D_{\mathbf{r}^{(1)}} E^{(1)} \circ W^{(1)}) \mathbf{x}) \\ &= \text{ReLU}(D_{\mathbf{r}^{(1)}} W^{(1)} \mathbf{x}) = \text{ReLU}(\mathbf{r}^{(1)} \circ (W^{(1)} \mathbf{x})) \\ &\stackrel{(a)}{=} \mathbf{r}^{(1)} \circ \text{ReLU}(W^{(1)} \mathbf{x}) = \mathbf{r}^{(1)} \circ \mathbf{y}^{(1)}, \end{aligned}$$

where (a) follows from the condition  $\mathbf{r}^{(1)} \in R_{>0}^{n_1}$ .

Then, for  $2 \leq l \leq L-1$ , assuming  $\hat{\mathbf{y}}^{(l-1)} = \mathbf{r}^{(l-1)} \circ \mathbf{y}^{(l-1)}$  by induction, we have

$$\begin{aligned} \hat{\mathbf{y}}^{(l)} &= \text{ReLU}(\widehat{W}^{(l)} \hat{\mathbf{y}}^{(l-1)}) \\ &= \text{ReLU}((R^{(l)} \circ W^{(l)}) (\mathbf{r}^{(l-1)} \circ \mathbf{y}^{(l-1)})) \\ &= \text{ReLU}((R^{(l)} \circ W^{(l)}) D_{\mathbf{r}^{(l-1)}} \mathbf{y}^{(l-1)}) \\ &= \text{ReLU}(((R^{(l)} D_{\mathbf{r}^{(l-1)}}) \circ W^{(l)}) \mathbf{y}^{(l-1)}) \\ &= \text{ReLU}((D_{\mathbf{r}^{(l)}} E^{(l)} \circ W^{(l)}) \mathbf{y}^{(l-1)}) \\ &= \text{ReLU}(D_{\mathbf{r}^{(l)}} W^{(l)} \mathbf{y}^{(l-1)}) = \text{ReLU}(D_{\mathbf{r}^{(l)}} \mathbf{z}^{(l)}) \\ &= \text{ReLU}(\mathbf{r}^{(l)} \circ \mathbf{z}^{(l)}) = \mathbf{r}^{(l)} \circ \mathbf{y}^{(l)}. \end{aligned}$$

Thus the Eq. (10) is proved. Furthermore, we have

$$\begin{aligned} \hat{\mathbf{y}}^{(L)} &= \widehat{W}^{(L)} \hat{\mathbf{y}}^{(L-1)} = (R^{(L)} \circ W^{(L-1)} + R^a) \hat{\mathbf{y}}^{(L-1)} \\ &= (R^{(L)} \circ W^{(L)}) (\mathbf{r}^{(L-1)} \circ \mathbf{y}^{(L-1)}) + R^a \hat{\mathbf{y}}^{(L-1)} \\ &= (R^{(L)} D_{\mathbf{r}^{(L-1)}}) \circ W^{(L)} \mathbf{y}^{(L-1)} + R^a \hat{\mathbf{y}}^{(L-1)} \\ &= (E^{(L)} \circ W^{(L)}) \mathbf{y}^{(L-1)} + R^a \hat{\mathbf{y}}^{(L-1)} \\ &= W^{(L)} \mathbf{y}^{(L-1)} + R^a \hat{\mathbf{y}}^{(L-1)} \\ &= \mathbf{y}^{(L)} + \gamma \alpha \mathbf{r}_a = \mathbf{y}^{(L)} + \alpha \mathbf{r}. \end{aligned}$$

□

### 3.1.2. CONVOLUTIONAL NEURAL NETWORKS

Convolutional Neural Networks (CNN) have proven to be effective in many computer vision and natural language processing tasks. In this section, we continue to demonstrate how to apply our encryption method to CNNs.

Although convolution operation can be applied to any dimensional input, we focus on 3-dimensional inputs since we are most concerned about image data. For any input  $I^{(l)} \in \mathbb{R}^{c_l \times h_l \times w_l}$ , where  $c_l$ ,  $w_l$  and  $h_l$  are the number of channels, weight and height, respectively, the convolution operation, denoted by  $I^{(l+1)} = I^{(l)} * W^{(l)}$ , is defined as

$$I_{k,i,j}^{(l+1)} = \sum_{c'=1}^{c_l} \sum_{i'=1}^f \sum_{j'=1}^f W_{k,c',i',j'}^{(l)} I_{c',i+i',j+j'}^{(l)}$$

where  $W^{(l+1)} \in \mathbb{R}^{c_{l+1} \times c_l \times f \times f}$  is a set of  $c_{l+1}$  filters with each filter of shape  $c_l \times f \times f$ , and  $I^{(l+1)} \in \mathbb{R}^{c_{l+1} \times h_{l+1} \times w_{l+1}}$  is the output image.

From the above, convolutional layer can be implemented with a convolution operation followed by a non-linear function, and a CNN can be constructed by interweaving several convolutional and spatial pooling layers. At last, the CNN ends with a fully-connected layer for regression or classification tasks. In order to apply our encryption method to CNNs, we choose ReLU as the non-linear function and MaxPooling as the spatial pooling layer. In fact, (Ma & Lu, 2017) proved the equivalence of convolutional and fully connected operations. Therefore, the multiplicative noise introduced for MLP will not affect the operation of convolutional layers, which can be adopted with small alteration.

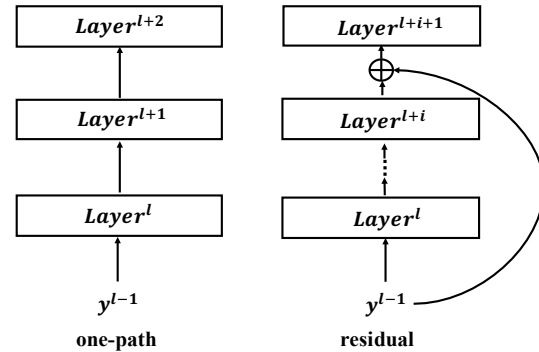


Figure 2. Common connections in neural networks.  $\oplus$  can be element-wise summation, element-wise multiplication or concatenation. In this paper we choose concatenation.

Section 3.1.1 mainly discusses about the “one-path” connection, i.e., the input of  $l$ -th layer is exactly the output of  $(l-1)$ -th layer. Most state-of-the-art CNN models, e.g., ResNet (He et al., 2016) and DenseNet (Huang et al., 2017), however, utilize residual connections in their structures, i.e.,

the  $l$ -th layer takes the output of the multiple precedent layers as input, as illustrated in Fig. 2. There are various kind of residual connections, for simplicity, we choose to connect the precedent outputs over the channel dimension.

**1. Parameter encryption.** Similar to Section 3.1.1, the server first randomly selects the multiplicative noisy vector  $\mathbf{r}^{(l)} \in \mathbb{R}_{>0}^{c_l}$  for  $1 \leq l \leq L-1$ , the additive noisy vector  $\mathbf{r}_a \in \mathbb{R}^{n_L}$  with pairwise different components, and a random coefficient  $\gamma \in \mathbb{R}$ . Then, the server computes

$$\widehat{W}^{(l)} = \begin{cases} R^{(l)} \circ W^{(l)}, & \text{for } 1 \leq l \leq L-1, \\ R^{(L)} \circ W^{(L)} + R^a, & \text{for } l = L, \end{cases} \quad (12)$$

where  $R^{(l)} \in \mathbb{R}^{c_l \times c_{l-1} \times f \times f}$  for  $l \in [1, L-1]$ , satisfies

$$R_{k,c',i',j'}^{(l)} = \begin{cases} \mathbf{r}_k^{(l)}, & \text{when } l = 1, \\ \mathbf{r}_k^{(l)} / \mathbf{r}_{c'}^{(l, in)} & \text{when } 2 \leq l \leq L-1. \end{cases} \quad (13)$$

where  $k \in [1, c_l]$ ,  $c' \in [1, c_{l-1}]$ ,  $i' \in [1, f]$  and  $j' \in [1, f]$ .  $\mathbf{r}^{(l, in)} = (\mathbf{r}^{(m)})_{m \in P(l)}$  is the concatenate vector of all vectors  $\mathbf{r}^{(m)}$  for  $m \in P(l)$ , and  $P(l)$  denotes the set of layers connected with the  $l$ -th layer.  $R^L, R^a \in \mathbb{R}^{n_L \times (c_{L-1} h_{L-1} w_{L-1})}$  satisfy

$$R_{ij}^{(L)} = 1 / \mathbf{r}_{[j/(h_{L-1} w_{L-1})]}^{(L-1)}. \quad (14)$$

$$R_{ij}^a = \gamma \cdot \mathbf{r}_{a,i} \quad (15)$$

where  $i \in [1, n_L]$  and  $j \in [1, n_{L-1}]$ .

It is worth noting that compared with the noisy vector of MLP, we can ignore the spatial dimensions (i.e., height and width) and just impose the same noisy value on them.

**2. Forward propagation.** Similar to the MLP, each client computes the noisy output of each layer as follows.

(1) For the  $l$ -th layer, where  $l = 1, 2, \dots, L-1$ , the corresponding noisy output  $\hat{I}_k^{(l)}$  is a matrix for the  $k$ -th channel, where each element in  $\hat{I}_k^{(l)}$  is represented as

$$\hat{I}_{k,i',j'}^{(l)} = \mathbf{r}_k^{(l)} \hat{I}_{k,i',j'}^{(l)}. \quad (16)$$

(2) For the last fully connected layer, the final noisy prediction vector  $\hat{\mathbf{y}}^{(L)}$  is computed as

$$\hat{\mathbf{y}}^{(L)} = \mathbf{y}^{(L)} + \gamma \alpha \mathbf{r}_a = \mathbf{y}^{(L)} + \alpha \mathbf{r}, \quad (17)$$

where  $\alpha = \sum_{j=1}^{n_{L-1}} \text{Flatten}(\hat{I}^{(L-1)})_j$ , and the  $\text{Flatten}(\hat{I}^{(L-1)})$  means expanding  $\hat{I}^{(L-1)}$  into a vector along the channel, height and width dimensions, which implies  $n_{L-1} = c_{L-1} h_{L-1} w_{L-1}$ .

Since the derivations of output in the CNN are similar to the MLP, due to the space limitation, we omit the derivations of Eqs. (16) and (17) here, and the details can be found in the attachment.

### 3.2. Noisy Gradient Computation

Generally, the local training performed by each client includes the forward propagation and backward propagation. Since the forward propagation has been introduced in Section 3.1, we just show the backward propagation here, i.e., noisy gradient computation<sup>2</sup>. More specifically, after obtain the noisy outputs of each layer in forward propagation process, i.e.,  $\hat{\mathbf{y}}^{(l)}$  for  $l = 1, 2, \dots, L$ , the client calculates the corresponding gradients based on the MSE loss function (see Eq. (3)<sup>3</sup>). Considering our encrypted model, for each sample  $(\mathbf{x}, \bar{\mathbf{y}})$ , from Lemma 1, the noisy MSE is

$$\hat{\mathcal{L}} = \frac{1}{2} \sum_{i=1}^{n_L} (\hat{\mathbf{y}}_i^{(L)} - \bar{\mathbf{y}}_i)^2 = \frac{1}{2} \sum_{i=1}^{n_L} (\mathbf{y}_i^{(L)} - \bar{\mathbf{y}}_i + \alpha \mathbf{r}_i)^2.$$

In what follows, we give the relation between the noisy gradients and the true gradients.

**Lemma 2.** For any  $1 \leq l \leq L$ , the noisy gradient matrix  $\frac{\partial \hat{\mathcal{L}}}{\partial \widehat{W}^{(l)}}$  and the true gradient matrix  $\frac{\partial \mathcal{L}}{\partial W^{(l)}}$  satisfy

$$\frac{\partial \hat{\mathcal{L}}}{\partial \widehat{W}^{(l)}} = \frac{1}{R^{(l)}} \circ \frac{\partial \mathcal{L}}{\partial W^{(l)}} + \gamma \boldsymbol{\sigma}^{(l)} - v \boldsymbol{\beta}^{(l)} \quad (18)$$

where  $\boldsymbol{\sigma}^{(l)} = \mathbf{r}_a^T \left( \alpha \frac{\partial \hat{\mathbf{y}}^{(L)}}{\partial \widehat{W}^{(l)}} + \left( \frac{\partial \hat{\mathcal{L}}}{\partial \hat{\mathbf{y}}^{(L)}} \right)^T \frac{\partial \alpha}{\partial \widehat{W}^{(l)}} \right)$ ,  $v = \mathbf{r}^T \mathbf{r}$  and  $\boldsymbol{\beta}^{(l)} = \alpha \frac{\partial \alpha}{\partial \widehat{W}^{(l)}}$ .

*Proof.* Based on the noisy MSE, we have

$$\frac{\partial \hat{\mathcal{L}}}{\partial \hat{\mathbf{y}}^{(L)}} = (\hat{\mathbf{y}}^{(L)} - \bar{\mathbf{y}})^T = \frac{\partial \mathcal{L}}{\partial \mathbf{y}^{(L)}} + \alpha \mathbf{r}^T,$$

Thus, we can derive that

$$\begin{aligned} \frac{\partial \hat{\mathcal{L}}}{\partial \widehat{W}^{(l)}} &= \frac{\partial \hat{\mathcal{L}}}{\partial \hat{\mathbf{y}}^{(L)}} \frac{\partial \hat{\mathbf{y}}^{(L)}}{\partial \widehat{W}^{(l)}} = \left( \frac{\partial \mathcal{L}}{\partial \mathbf{y}^{(L)}} + \alpha \mathbf{r}^T \right) \frac{\partial \hat{\mathbf{y}}^{(L)}}{\partial \widehat{W}^{(l)}} \\ &= \frac{\partial \mathcal{L}}{\partial \mathbf{y}^{(L)}} \left( \frac{\partial \mathbf{y}^{(L)}}{\partial W^{(l)}} + \frac{\partial (\alpha \mathbf{r})}{\partial W^{(l)}} \right) + \alpha \mathbf{r}^T \frac{\partial \hat{\mathbf{y}}^{(L)}}{\partial \widehat{W}^{(l)}} \\ &= \frac{\partial \mathcal{L}}{\partial \widehat{W}^{(l)}} + \left( \frac{\partial \hat{\mathcal{L}}}{\partial \hat{\mathbf{y}}^{(L)}} - \alpha \mathbf{r}^T \right) \frac{\partial (\alpha \mathbf{r})}{\partial \widehat{W}^{(l)}} + \alpha \mathbf{r}^T \frac{\partial \hat{\mathbf{y}}^{(L)}}{\partial \widehat{W}^{(l)}} \\ &= \frac{\partial \mathcal{L}}{\partial \widehat{W}^{(l)}} + \mathbf{r}^T \left( \alpha \frac{\partial \hat{\mathbf{y}}^{(L)}}{\partial \widehat{W}^{(l)}} + \left( \frac{\partial \hat{\mathcal{L}}}{\partial \hat{\mathbf{y}}^{(L)}} \right)^T \frac{\partial \alpha}{\partial \widehat{W}^{(l)}} \right) \\ &\quad - v \alpha \frac{\partial \alpha}{\partial \widehat{W}^{(l)}} \\ &= \frac{1}{R^{(l)}} \circ \frac{\partial \mathcal{L}}{\partial W^{(l)}} + \gamma \boldsymbol{\sigma}^{(l)} - v \boldsymbol{\beta}^{(l)}. \end{aligned}$$

□

<sup>2</sup> The derivations given in the following contents can be applied in both MLP and CNN.

<sup>3</sup> Unless other specification, we use  $\mathcal{L}$  to represent  $\mathcal{L}(W; (\mathbf{x}_i, \bar{\mathbf{y}}_i))$  as shorthand in the rest of this paper.



Note that  $\sigma^{(l)}$  and  $\beta^{(l)}$  can be computed directly by the clients. For all samples in the mini-batch dataset  $\mathcal{D}_k^t \in \mathcal{D}_k$ , the  $k$ -th client computes the average gradients and the noisy items:  $\frac{\partial \hat{\mathcal{L}}}{\partial W^{(l)}} = \frac{1}{|\mathcal{D}_k^t|} \sum_{n \in \mathcal{D}_k^t} \frac{\partial \hat{\mathcal{L}}_n}{\partial W^{(l)}}$ ,  $\sigma^{(l)} = \frac{1}{|\mathcal{D}_k^t|} \sum_{n \in \mathcal{D}_k^t} \sigma_n^{(l)}$  and  $\beta^{(l)} = \frac{1}{|\mathcal{D}_k^t|} \sum_{n \in \mathcal{D}_k^t} \beta_n^{(l)}$ . Finally, the  $k$ -th client returns  $\{\frac{\partial \hat{\mathcal{L}}}{\partial W^{(l)}}, \sigma^{(l)}, \beta^{(l)}\}_k$  to the server, for  $l = 1, 2, \dots, L$ .

### 3.3. Model Update

After receiving the noisy local gradients from all clients, the server can recover the true model updates for the next iteration (i.e.,  $(t+1)$ -th iteration) by Lemma 2.

**(1) Gradient recovery.** For the noisy local gradients of the  $k$ -th client, the server computes: for  $l = 1, 2, \dots, L$ ,

$$\nabla F_k(W_t^{(l)}) = R^{(l)} \circ \left( \frac{\partial \hat{\mathcal{L}}}{\partial \widehat{W}^{(l)}} - \gamma \cdot \sigma^{(l)} + v \beta^{(l)} \right). \quad (19)$$

**(2) Parameter aggregation.** Based on Eq. (4), the server aggregates all clients' local gradients to update the global model parameters for the  $(t+1)$ -th iteration as

$$W_{t+1}^{(l)} \leftarrow W_t^{(l)} - \eta \sum_k \frac{N_k}{N} \nabla F_k(W_t^{(l)}).$$

**Data Processing.** The server and all clients interactively iterate the processes in Sections 3.1-3.3 until the convergence. Consequently, the server obtains final model parameters  $W = \{W^{(l)}\}_{l=1}^L$ . In order to protect  $W$  and allow each client to use the model, the server still needs to encrypt  $W$ . Specifically, the operations are similar to that in Section 3.1, the only difference is that in the last layer, the server does not adopt the additive noises  $\mathbf{r}_a$  and  $\gamma$ . Thus, the noisy model parameters are computed

$$\widehat{W}^{(l)} = R^{(l)} \circ W^{(l)}, \text{ for } 1 \leq l \leq L.$$

Specifically,  $R^{(l)}$  satisfies Eq. (7) for the MLP, and satisfies Eqs. (13) and (14) for the CNN. Obviously, without the influence of additive noises  $\mathbf{r}_a$  and  $\gamma$ , based on Lemma 1 and Eq. (17), it can be verified that the final prediction is  $\hat{\mathbf{y}}^{(L)} = \mathbf{y}^{(L)}$ , i.e., the true prediction.

## 4. Security Analysis

Based on design goals, we analyze the security properties of our scheme in this section.

**(1) Privacy-preservation of model parameters.** Whether it is training or data processing, clients only possess the noisy model parameters, i.e.,  $\widehat{W} = \{\widehat{W}^{(l)}\}_{l=1}^L$ , where

$\widehat{W}^{(l)} = R^{(l)} \circ W^{(l)}$  and  $\widehat{W}^{(L)} = R^{(L)} \circ W^{(L)} + R^a$  (or  $\widehat{W}^{(L)} = R^{(L)} \circ W^{(L)}$  after training). Since the noisy matrices  $R^{(l)}$  and  $R^a$  are randomly chosen as the secret keys, the server keeps them and the original model parameters  $W^{(l)}$  secret from clients. For given  $\widehat{W}^{(l)}$ , there exist infinite pairs  $(R^{(l)}, W^{(l)})$  and infinite triples  $(R^{(L)}, R^a, W^{(L)})$  such that  $R^{(l)} \circ W^{(l)} = \widehat{W}^{(l)}$  and  $R^{(L)} \circ W^{(L)} + R^a = \widehat{W}^{(L)}$ . Therefore, clients cannot obtain the exact model parameters  $W$ , even in collusion with others.

**(2) Privacy-preservation of the true prediction in each iteration:** As shown in Section 3.1, the client computes the noisy prediction vector  $\hat{\mathbf{y}}^{(L)}$  as  $\mathbf{y}^{(L)} + \gamma \alpha \mathbf{r}_a$ , where  $\mathbf{y}^{(L)}$  is the true prediction vector. The parameter  $\alpha$  and noisy vector  $\mathbf{r}_a$  are known to the client, while  $\gamma$  is chosen by the server randomly which is unknown to the client.

**Lemma 3.** For any  $\hat{\mathbf{y}}_i^{(L)}$  and  $\hat{\mathbf{y}}_j^{(L)}$ , where  $1 \leq i \neq j \leq c$ , there exist infinite triples  $(\mathbf{y}_i^{(L)}, \mathbf{y}_j^{(L)}, \gamma)$  such that  $\mathbf{y}_i^{(L)} > \mathbf{y}_j^{(L)}$  and

$$\hat{\mathbf{y}}_i^{(L)} = \mathbf{y}_i^{(L)} + \gamma \alpha \mathbf{r}_{a,i} \text{ and } \hat{\mathbf{y}}_j^{(L)} = \mathbf{y}_j^{(L)} + \gamma \alpha \mathbf{r}_{a,j} \quad (20)$$

Similarly, there exist infinite triples  $(\mathbf{y}_i^{(L)}, \mathbf{y}_j^{(L)}, \gamma)$  such that  $\mathbf{y}_i^{(L)} < \mathbf{y}_j^{(L)}$  and Eq. (20) holds.

*Proof.* We only prove the first conclusion since the proof of the second conclusion is completely similar to the first one. Without loss of generality, we assume  $\mathbf{r}_{a,i} > \mathbf{r}_{a,j}$  and  $\alpha > 0$ , and let  $\gamma$  be any real number such that

$$\gamma < (\hat{\mathbf{y}}_i^{(L)} - \hat{\mathbf{y}}_j^{(L)}) / (\alpha(\mathbf{r}_{a,i} - \mathbf{r}_{a,j})).$$

We take  $\mathbf{y}_i^{(L)} = \hat{\mathbf{y}}_i^{(L)} - \gamma \alpha \mathbf{r}_{a,i}$  and  $\mathbf{y}_j^{(L)} = \hat{\mathbf{y}}_j^{(L)} - \gamma \alpha \mathbf{r}_{a,j}$ , then the Eq. (20) holds and  $\mathbf{y}_i^{(L)} - \mathbf{y}_j^{(L)} = \hat{\mathbf{y}}_i^{(L)} - \hat{\mathbf{y}}_j^{(L)} - \gamma \alpha(\mathbf{r}_{a,i} - \mathbf{r}_{a,j}) > 0$ .  $\square$

According to Lemma 3, for any  $1 \leq i \neq j \leq c$ , the clients cannot know whether  $\mathbf{y}_i^{(L)} > \mathbf{y}_j^{(L)}$  or  $\mathbf{y}_i^{(L)} < \mathbf{y}_j^{(L)}$ . Thus the clients cannot know the largest one in  $\mathbf{y}_1^{(L)}, \mathbf{y}_2^{(L)}, \dots, \mathbf{y}_c^{(L)}$ , i.e., they cannot obtain the true prediction.

From the above, there is no doubt that each clients also cannot know the true local gradients. In other words, each client can obtain neither the intermediate iterates nor final model parameters, let alone the training data of others.

**(3) Privacy-preservation of the raw training data of clients:** In order to help the server to recover true gradients, each client returns additional noisy terms  $\sigma^{(l)}$  and  $\beta^{(l)}$  to the server. Since  $\sigma^{(l)}$  and  $\beta^{(l)}$  are still combinations of some related gradients, they contain typically significantly

less additional information compared to the raw training data. Besides,  $\sigma^{(l)}$  and  $\beta^{(l)}$  are also affected by the ReLU non-linear activation. Thus these gradients will become complicated non-linear functions of the raw data. Similar to the traditional FL, resolving the raw data from additional noisy terms is as difficult as resolving from the gradients. In other words, our PBPFL can provide clients with the same level of privacy protection as the traditional FL.

In fact, our PBPFL can improve the privacy of local training data by adopting secret sharing technique. For example,  $K$  clients consult with a set of random numbers  $(\lambda_1, \lambda_2, \dots, \lambda_K)$  such that  $\sum_{k=1}^K \lambda_k = 0$ , which are unknown to the server. The  $k$ -th client holds  $\lambda_k$ , and after computing  $\frac{\partial \hat{\mathcal{L}}}{\partial W^{(l)}}$ ,  $\sigma^{(l)}$  and  $\beta^{(l)}$ , he or she adds  $\lambda_k$  to them. The server can only obtain the aggregated results rather than the individual gradient of each client. Since our main goal is to achieve the privacy-preservation of intermediate iterates and final model parameters, we do not delve into this approach, but will improve our PBPFL in future work.

## 5. Performance Evaluation

We empirically evaluate our PBPFL algorithm on real-world datasets, from two different perspectives: **effectiveness** (i.e., how well our algorithm perform on these datasets) and **efficiency** (i.e., how much extra computation and communication cost our method spends).

### 5.1. Experimental Setup

We implement our methods based on the native network layer in Pytorch (Paszke et al., 2019) running on single Tesla M40 GPU. We adopt FedAvg (McMahan et al., 2017) as the baseline algorithm for comparison. In all experiments, the training epochs and the batch-size of each client are set to be 200 and 32, respectively.

**Datasets and Metrics.** We evaluate our method on three privacy-sensitive datasets covering both the bank and medical scenarios.

**(1) UCI Bank Marketing Dataset (Moro et al., 2014)** (UBMD) is related to direct marketing campaigns of a Portuguese banking institution and aims to predict the possibility of clients for subscribing deposits. It contains 41188 instances of 17 dimensional bank data. Following conventional practise, we split the dataset into training/validation/test sets by 8:1:1. We adopt MSE as the evaluation metric.

**(2) APTOS Blindness Detection**<sup>4</sup> (ABD) consists of 3.6k training and 1.9k test datasets of retina images for predicting the severity of diabetic retinopathy. For preprocessing, we

center-crop images and resize them into size of  $64 \times 64$ . Again, we use MSE as the evaluation metric.

**(3) Lesion Disease Classification (Tschandl et al., 2018) (Codella et al., 2019)** (LDC) provides 8k training and 2k test skin images for the classification of lesion disease. We downsample the images into  $64 \times 64$  and adopt classification accuracy as the evaluation metric.

### 5.2. Empirical Results

We evaluate the training accuracy of our algorithm against native FedAvg on both regression and classification tasks. Besides, we present the computation and communication overhead of the basic building blocks in PBPFL.

#### 5.2.1. REGRESSION

We evaluate the performance of PBPFL on regression tasks with UBMD and LDC. For a more comprehensive comparison, we train ResNet20 and MLP with 3, 5 and 7 layers on ABD and UBMD, respectively. Also, we evaluate the performance for  $k = 1, 5, 10$  clients on both datasets. Table 1 shows the MSE for the final converged model on testsets.

From the table, the accuracy of PBPFL elegantly aligns with that of FedAvg under various settings, which verifies our derivation in Section 3. Although some operations (e.g., dividing by random vectors) may cause precision errors, we find those have little impact on the training procedure.

Table 1. MSE Result for regression tasks. Lower MSE means better performance.

			$k = 1$	$k = 5$	$k = 10$
UBMD	FedAvg	MLP-3	0.059	0.079	0.097
		MLP-5	0.059	0.079	0.100
		MLP-7	0.058	0.086	0.113
	PBPFL	MLP-3	0.060	0.078	0.097
		MLP-5	0.059	0.077	0.101
		MLP-7	0.059	0.082	0.114
ABD	FedAvg	ResNet20	0.048	0.085	0.117
	PBPFL	ResNet20	0.047	0.088	0.114

#### 5.2.2. CLASSIFICATION

In this section, we evaluate PBPFL for the classification task with ResNet20 models. Note that the MSE loss is not primarily designed for classification tasks, thus, we evaluate the accuracy of FedAvg by adopting both MSE loss (denoted as FedAvg-MSE) and cross-entropy loss (denoted as FedAvg-CE) as baselines. The accuracy of converged models on testsets is shown in Tab. 2.

Similar to regression tasks, the accuracy of PBPFL elegantly aligns with FedAvg-MSE. Compared to FedAvg-CE adopting a more suitable loss for classification, PBPFL suffers from an acceptable accuracy loss, i.e., decreased by 0.67, 3.2, 2.11 when the client number is 1, 5, 10 respectively.

<sup>4</sup><https://www.kaggle.com/c/aptos2019-blindness-detection>

Table 2. Accuracy result for classification task.

		$k = 1$	$k = 5$	$k = 10$
LDC	FEDAVG-CE	66.90	64.93	63.38
	FEDAVG-MSE	66.24	61.68	61.44
	PBPFL	66.23	61.74	61.27

### 5.2.3. COMMUNICATION AND COMPUTATION

We dive into each of the components of PBPFL and compare computation and communication overheads of our method with FedAvg. The experiments are conducted on ResNet56 with an input size of  $224 \times 224$ , a batch size of 32 and iteration number of 250.

Tab. 3 shows the comparison of computational cost for PBPFL and FedAvg. **PP**, **LFP**, **LBP**, and **MU** stands for parameter perturbation, local forward propagation, local backward propagation and model update, respectively. From the table, we can see compared to FedAvg, the computational cost of PBPFL has approximately doubled, which is mainly caused by the backward propagation on client side (i.e., 91.08 to 228.06 seconds). This is due to the computation of additional information, i.e.  $\sigma$  and  $\beta$ , for noisy gradient recovery. The increased cost of PBPFL on the server side is basically negligible, indicating the server can afford the FL as usual.

Table 3. Computational overhead of PBPFL (Seconds).

		PP	LFP	LBP	MU	Total
FedAvg	Client	0	2.19	88.89	0	91.08
	Server	0	0	0	89.11	89.11
PBPFL	Client	0	2.20	225.86	0	228.06
	Server	3.66	0	0	92.39	96.05

The communication overhead mainly includes two interactions: the server sends noisy parameters  $\widehat{W} = \{\widehat{W}^{(l)}\}_{l=1}^L$  together with the  $c$ -dimensional noisy vector  $\mathbf{r}_a$  to clients and each client returns local noisy gradients  $\{\frac{\partial \widehat{\mathcal{L}}}{\partial \widehat{W}^{(l)}}\}_{l=1}^L$  together with two extra noisy items  $\{\sigma^{(l)}, \beta^{(l)}\}_{l=1}^L$ . Obviously, compared to FedAvg, the added communication costs are  $\mathbf{r}_a$  and  $\{\sigma^{(l)}, \beta^{(l)}\}_{l=1}^L$ , where the cost of  $\mathbf{r}_a$  can be negligible. Therefore, theoretical analysis shows that the additional communication is  $\mathcal{O}(2|W|)$ , where  $|W|$  is the size of model parameters. The experiments also confirm our theoretical results. Particularly, both the server-to-client and client-to-server communication overheads in FedAvg are 0.85 MB, while the server-to-client and client-to-server communication overheads in PBPFL are 0.85 MB and 2.55 MB, respectively.

In summary, in order to achieve the privacy preservation, we bring about certain amount of extra computation and communication costs. Nonetheless, we try the best to decrease the additional cost and keep it in constant level without

decreasing the model accuracy compared to the original FL.

## 6. Related Work

Federated learning was formally introduced by Google in 2016 (Konecny et al., 2016) to address the data privacy in machine learning. Then, FedAvg (McMahan et al., 2017) and its theoretical research (Li et al., 2019c) were introduced to implement and flourish FL. After that, many improvements and variants of FedAvg were deployed to deal with statistical challenges (Smith et al., 2017; Eichner et al., 2019; Mohri et al., 2019), communication challenges (Agarwal et al., 2018; Zhu & Jin, 2019; Chen et al., 2019) and privacy issues (Bonawitz et al., 2017; Xu et al., 2020; Li et al., 2019b; Bonawitz et al., 2016). Considering the potential value of federal learning, many promising applications, such as healthcare (Li et al., 2019b; Xu & Wang, 2019), virtual keyboard prediction (Ramaswamy et al., 2019; Yang et al.) and vehicle-to-vehicle communication (Samarakoon et al., 2018), have tried to adopt FL as an innovative mechanism to train global model from multiple parties with privacy-preserving property.

Recently, some summary works on FL have been presented (Dai et al., 2018; Yang et al., 2019; Li et al., 2019a; Kairouz et al., 2019). Specifically, Dai et al. (Dai et al., 2018) provided an overview of the architecture and optimization approach for federated data analysis. Yang et al. (Yang et al., 2019) identified architectures for the FL framework and summarized general privacy-preserving techniques that can be applied to FL. Li et al. (Li et al., 2019a) provided a broad overview of current approaches and outlined several directions of future work of FL. Peter et al. (Kairouz et al., 2019) outlined the classification of FL and discussed recent advances and presented an extensive collection of open problems and challenges.

From the above, it is still a big challenge to effectively protect the intermediate iterates during the training phase and the final model parameters in FL (Kairouz et al., 2019).

## 7. Conclusion

In this paper, we present a practical and bilateral privacy-preserving federated learning scheme, which aims to protect model iterates and final model parameters from disclosing. We introduce an efficient privacy-preserving technique to encrypt model iterates and final model parameters. This technique allows clients to train the updated model under noisy current model, and more importantly, ensures only the server can eliminate the noise to get accurate results. Security analysis shows the high security of our PBPFL under the honest but curious security setting. Besides, experiments conducted on real data also demonstrate the practical performance of our PBPFL.



## References

- Agarwal, N., Suresh, A. T., Yu, F. X., Kumar, S., and McMahan, B. cpsgd: Communication-efficient and differentially-private distributed SGD. In *NeurIPS*, 2018.
- Bonawitz, K., Ivanov, V., Kreuter, B., Marcedone, A., McMahan, H. B., Patel, S., Ramage, D., Segal, A., and Seth, K. Practical secure aggregation for federated learning on user-held data. In *Advances in Neural Information Processing Systems - 30th NeurIPS Workshop on Private Multi-Party Machine Learning, (NeurIPS 2016)*, 2016.
- Bonawitz, K., Ivanov, V., Kreuter, B., Marcedone, A., McMahan, H. B., Patel, S., Ramage, D., Segal, A., and Seth, K. Practical secure aggregation for privacy-preserving machine learning. In *CCS*, 2017.
- Chen, Y., Sun, X., and Jin, Y. Communication-efficient federated deep learning with asynchronous model update and temporally weighted aggregation. *CoRR*, 2019.
- Codella, N. C. F., Rotemberg, V., Tschandl, P., Celebi, M. E., Dusza, S. W., Gutman, D., Helba, B., Kalloo, A., Liopyris, K., Marchetti, M. A., Kittler, H., and Halpern, A. Skin lesion analysis toward melanoma detection 2018: A challenge hosted by the international skin imaging collaboration (ISIC). *CoRR*, 2019.
- Dai, W., Wang, S., Xiong, H., and Jiang, X. Privacy preserving federated big data analysis. In *Guide to Big Data Applications*. 2018.
- Dwork, C., Kenthapadi, K., McSherry, F., Mironov, I., and Naor, M. Our data, ourselves: Privacy via distributed noise generation. In *EUROCRYPT*, 2006.
- Eichner, H., Koren, T., McMahan, B., Srebro, N., and Talwar, K. Semi-cyclic stochastic gradient descent. In *ICML*, 2019.
- He, K., Zhang, X., Ren, S., and Sun, J. Deep residual learning for image recognition. In *CVPR*, 2016.
- Hitaj, B., Ateniese, G., and Pérez-Cruz, F. Deep models under the GAN: information leakage from collaborative deep learning. In *CCS*, 2017.
- Horn, R. A. and Johnson, C. R. *Matrix Analysis*, 2nd Ed. Cambridge University Press, 2012.
- Huang, G., Liu, Z., van der Maaten, L., and Weinberger, K. Q. Densely connected convolutional networks. In *CVPR*, 2017.
- Kairouz, P., McMahan, H. B., Avent, B., Bellet, A., Bennis, M., and et al. Advances and open problems in federated learning. *hal-02406503*, 2019.
- Konečný, J., McMahan, H. B., Yu, F. X., Richtárik, P., Suresh, A. T., and Bacon, D. Federated learning: Strategies for improving communication efficiency. *CoRR*, 2016.
- Li, T., Sahu, A. K., Talwalkar, A., and Smith, V. Federated learning: Challenges, methods, and future directions. *CoRR*, 2019a.
- Li, W., Milletari, F., Xu, D., Rieke, N., Hancox, J., Zhu, W., Baust, M., Cheng, Y., Ourselin, S., Cardoso, M. J., and Feng, A. Privacy-preserving federated brain tumour segmentation. In *Machine Learning in Medical Imaging - 10th International Workshop, (MLMI 2019)*, 2019b.
- Li, X., Huang, K., Yang, W., Wang, S., and Zhang, Z. On the convergence of fedavg on non-iid data. In *Proceedings of International Conference on Learning Representations (ICLR 2020)*, 2019c.
- Liu, X., Lu, R., Ma, J., Chen, L., and Qin, B. Privacy-preserving patient-centric clinical decision support system on naïve bayesian classification. *IEEE J. Biomedical and Health Informatics*, 2016.
- Ma, W. and Lu, J. An equivalence of fully connected layer and convolutional layer. *CoRR*, 2017.
- McMahan, B., Moore, E., Ramage, D., Hampson, S., and y Arcas, B. A. Communication-efficient learning of deep networks from decentralized data. In *Proceedings of the 20th International Conference on Artificial Intelligence and Statistics, (AISTATS 2017)*, 2017.
- Mohri, M., Sivek, G., and Suresh, A. T. Agnostic federated learning. In *ICML*, 2019.
- Moro, S., Cortez, P., and Rita, P. A data-driven approach to predict the success of bank telemarketing. *Decision Support Systems*, 2014.
- Paszke, A., Gross, S., Massa, F., Lerer, A., Bradbury, J., Chanan, G., Killeen, T., Lin, Z., Gimelshein, N., Antiga, L., Desmaison, A., Köpf, A., Yang, E., DeVito, Z., Raison, M., Tejani, A., Chilamkurthy, S., Steiner, B., Fang, L., Bai, J., and Chintala, S. Pytorch: An imperative style, high-performance deep learning library. In Wallach, H. M., Larochelle, H., Beygelzimer, A., d'Alché-Buc, F., Fox, E. B., and Garnett, R. (eds.), *NeurIPS*, 2019.
- Phong, L. T., Aono, Y., Hayashi, T., Wang, L., and Moriai, S. Privacy-preserving deep learning via additively homomorphic encryption. *IEEE Trans. Information Forensics and Security*, 2018.
- Ramaswamy, S., Mathews, R., Rao, K., and Beaufays, F. Federated learning for emoji prediction in a mobile keyboard. *CoRR*, 2019.

- Samarakoon, S., Bennis, M., Saad, W., and Debbah, M. Federated learning for ultra-reliable low-latency V2V communications. In *GLOBECOM*, 2018.
- Smith, V., Chiang, C., Sanjabi, M., and Talwalkar, A. S. Federated multi-task learning. In *NeurIPS*, 2017.
- Tschandl, P., Rosendahl, C., and Kittler, H. The HAM10000 dataset: A large collection of multi-source dermatoscopic images of common pigmented skin lesions. *CoRR*, 2018.
- Wikipedia. Facebook-cambridge analytica data scandal. [https://en.wikipedia.org/wiki/Facebook%E2%80%93Cambridge\\_Analytica\\_data\\_scandal](https://en.wikipedia.org/wiki/Facebook%E2%80%93Cambridge_Analytica_data_scandal), 2018.
- Xu, G., Li, H., Liu, S., Yang, K., and Lin, X. Verifynet: Secure and verifiable federated learning. *IEEE Trans. Information Forensics and Security*, 2020.
- Xu, J. and Wang, F. Federated learning for healthcare informatics. *CoRR*, 2019.
- Yang, Q., Liu, Y., Chen, T., and Tong, Y. Federated machine learning: Concept and applications. *ACM TIST*, 2019.
- Yang, T., Andrew, G., Eichner, H., Sun, H., Li, W., Kong, N., Ramage, D., and Beaufays, F. Applied federated learning: Improving google keyboard query suggestions. *CoRR*.
- Zhu, H. and Jin, Y. Multi-objective evolutionary federated learning. *IEEE transactions on neural networks and learning systems*, 2019.

---

## Appendix:

# Practical and Bilateral Privacy-preserving Federated Learning

---

### Abstract

This is the supplementary file of ICML 2020 submission: ID-409: Practical and Bilateral Privacy-preserving Federated Learning. The appendix contains the proofs for the noisy outputs of forward propagation in CNN and security analysis for the raw training data of clients in the proposed PBPFL. Then, an extended PBPFL is introduced to further improve privacy-preservation of the raw training data. Finally, the additional performance comparison between our PBPFL and the traditional FL, e.g., FedAvg, is also illustrated.

## A. Proofs for The Noisy Outputs of Forward Propagation in CNN.

### A.1. Proof of Eq. (16).

For the  $l$ -th layer, where  $l = 1, 2, \dots, L - 1$ , the corresponding noisy output  $\hat{I}_k^{(l)}$  is a matrix for the  $k$ -th channel, where each element in  $\hat{I}_k^{(l)}$  is represented as

$$\hat{I}_{k,i',j'}^{(l)} = \mathbf{r}_k^{(l)} I_{k,i',j'}^{(l)}. \quad (16)$$

*Proof.* As defined in Section 3.1.2, the convolutional layer is implemented as a convolution operation followed by a ReLU. Due to the existence of residual connection, the  $l$ -th layer may be connected to a set of preceding layers, denoted as  $P(l)$ . Obviously, the input of the  $l$ -th convolutional layer, denoted as  $I^{(l,in)} \in \mathbb{R}^{c_l, in \times h_l, in \times w_l, in}$ , is the concatenation of the output of layers in set  $P(l)$  along the channel dimension, which can be represented as

$$I^{(l,in)} = \underbrace{\left[ I_{1,i,j}^{(m)}, I_{2,i,j}^{(m)}; \dots; I_{c_m,i,j}^{(m)} \right]_{m \in P(l)}}_{\text{Concatenation along the channel dimension}}.$$

For example, if the 5-th layer is connected to layers 1, 2 and 4, then we have  $P(5) = \{1, 2, 4\}$  and

$$I^{(5,in)} = \left[ I_{1,i,j}^{(1)}; I_{2,i,j}^{(1)}; \dots; I_{c_1,i,j}^{(1)}; I_{1,i,j}^{(2)}; I_{2,i,j}^{(2)}; \dots; I_{c_2,i,j}^{(2)}; I_{1,i,j}^{(4)}; I_{2,i,j}^{(4)}; \dots; I_{c_4,i,j}^{(4)} \right].$$

Therefore, the output of the  $l$ -th convolutional layer  $I^{(l)} \in \mathbb{R}^{c_l \times h_l \times w_l}$  is defined as:

$$I_{k,i,j}^{(l)} = \text{ReLU} \left( \sum_{c'=1}^{c_{l,in}} \sum_{i'=1}^f \sum_{j'=1}^f W_{k,c',i',j'}^{(l)} I_{c',i+i',j+j'}^{(l,in)} \right),$$

where  $W^{(l)} \in \mathbb{R}^{c_l \times c_{l,in} \times f \times f}$  is the parameter of the  $l$ -th layer.

In what follows, we prove Eq. (16) by induction. More specifically, when  $l = 1$ , we have

$$\begin{aligned} \hat{I}_{k,i,j}^{(1)} &= \text{ReLU} \left( \sum_{c'=1}^{c_{1,in}} \sum_{i'=1}^f \sum_{j'=1}^f \widehat{W}_{k,c',i',j'}^{(1)} I_{c',i+i',j+j'}^{(1,in)} \right) \\ &= \text{ReLU} \left( \sum_{c'=1}^{c_{1,in}} \sum_{i'=1}^f \sum_{j'=1}^f \left( R_{k,c',i',j'}^{(1)} W_{k,c',i',j'}^{(1)} \right) I_{c',i+i',j+j'}^{(1,in)} \right) \end{aligned}$$

$$\begin{aligned}
 &= ReLU \left( \sum_{c'=1}^{c_{1,in}} \sum_{i'=1}^f \sum_{j'=1}^f \mathbf{r}_k^{(1)} W_{k,c',i',j'}^{(1)} I_{c',i+i',j+j'}^{(1,in)} \right) \\
 &= \mathbf{r}_k^{(1)} ReLU \left( \sum_{c'=1}^{c_{1,in}} \sum_{i'=1}^f \sum_{j'=1}^f W_{k,c',i',j'}^{(1)} I_{c',i+i',j+j'}^{(1,in)} \right) \\
 &= \mathbf{r}_k^{(1)} I_{k,i,j}^{(1)}.
 \end{aligned}$$

Then, for  $2 \leq l \leq L-1$ , assuming we have  $\hat{I}_{k,i,j}^{(h)} = \mathbf{r}_k^{(h)} I_{k,i,j}^{(h)}$ ,  $h = 1, 2, \dots, l-1$  by induction.

Obviously, by the definition of  $I^{(l,in)}$  ( $\hat{I}^{(l,in)}$ ), we can deduce that

$$\hat{I}_{k,i,j}^{(l,in)} = \mathbf{r}_k^{(l,in)} I_{k,i,j}^{(l,in)}$$

Then the noisy output of the  $l$ -th layer can be computed as

$$\begin{aligned}
 \hat{I}_{k,i,j}^{(l)} &= ReLU \left( \sum_{c'=1}^{c_{l,in}} \sum_{i'=1}^f \sum_{j'=1}^f \widehat{W}_{k,c',i',j'}^{(l)} \hat{I}_{c',i+i',j+j'}^{(l,in)} \right) \\
 &= ReLU \left( \sum_{c'=1}^{c_{l,in}} \sum_{i'=1}^f \sum_{j'=1}^f \left( R_{k,c',i',j'}^{(l)} W_{k,c',i',j'}^{(l)} \right) \mathbf{r}_{c'}^{(l,in)} I_{c',i+i',j+j'}^{(l,in)} \right) \\
 &= ReLU \left( \sum_{c'=1}^{c_{l,in}} \sum_{i'=1}^f \sum_{j'=1}^f \mathbf{r}_k^{(l)} / \mathbf{r}_{c'}^{(l,in)} \mathbf{r}_{c'}^{(l,in)} W_{k,c',i',j'}^{(l)} I_{c',i+i',j+j'}^{(l,in)} \right) \\
 &= \mathbf{r}_k^{(l)} ReLU \left( \sum_{c'=1}^{c_{l,in}} \sum_{i'=1}^f \sum_{j'=1}^f W_{k,c',i',j'}^{(l)} I_{c',i+i',j+j'}^{(l,in)} \right) \\
 &= \mathbf{r}_k^{(l)} I_{k,i,j}^{(l)}.
 \end{aligned}$$

□

## A.2. Proof of Eq. (17).

For the last fully connected layer, the final noisy prediction vector  $\hat{\mathbf{y}}^{(L)}$  is computed as

$$\hat{\mathbf{y}}^{(L)} = \mathbf{y}^{(L)} + \gamma \alpha \mathbf{r}_a = \mathbf{y}^{(L)} + \alpha \mathbf{r}, \quad (17)$$

where  $\alpha = \sum_{j=1}^{n_{L-1}} Flatten(\hat{I}^{(L-1)})_j$ , and the  $Flatten(\hat{I}^{(L-1)})$  means expanding  $\hat{I}^{(L-1)}$  into a vector along the channel, height and width dimensions, which implies  $n_{L-1} = c_{L-1} h_{L-1} w_{L-1}$ .

*Proof.* Let a vector  $\mathbf{y}^{(l)} \in \mathbb{R}^{c_l h_l w_l}$  be the flatten result of  $I^{(l)}$ , i.e.,  $\mathbf{y}_{kij}^{(l)} = I_{k,i,j}^{(l)}$ . Based on Eq. (16), we have

$$\hat{\mathbf{y}}_{kij}^{(L-1)} = \hat{I}_{k,i,j}^{(L-1)} = \mathbf{r}_k^{(L-1)} I_{k,i,j}^{(L-1)} = \mathbf{r}_k^{(L-1)} \mathbf{y}_{kij}^{(L-1)}$$

Denote  $n_l = c_l h_l w_l$ , then the output of last fully connected layer  $\hat{\mathbf{y}}_i^{(L)}$ , where  $i = 1, 2, \dots, n_L$ , can be computed as

$$\begin{aligned}
 \hat{\mathbf{y}}_i^{(L)} &= \sum_{j=1}^{n_{L-1}} \widehat{W}_{ij}^{(L)} \hat{\mathbf{y}}_j^{(L-1)} = \sum_{j=1}^{n_{L-1}} \left( R_{ij}^{(L)} W_{ij}^{(L)} + R_{ij}^a \right) \mathbf{r}_{\lfloor j/(h_{L-1} w_{L-1}) \rfloor}^{(L-1)} \mathbf{y}_j^{(L-1)} \\
 &= \sum_{j=1}^{n_{L-1}} \left( R_{ij}^{(L)} W_{ij}^{(L)} \mathbf{r}_{\lfloor j/(h_{L-1} w_{L-1}) \rfloor}^{(L-1)} \mathbf{y}_j^{(L-1)} + R_{ij}^a \hat{\mathbf{y}}_j^{(L-1)} \right)
 \end{aligned}$$



$$\begin{aligned}
 &= \sum_{j=1}^{n_{L-1}} \left( 1/r_{[j/(h_{L-1}w_{L-1})]} W_{ij}^{(L)} r_{[j/(h_{L-1}w_{L-1})]} y_j^{(L-1)} \right) + \sum_{j=1}^{n_{L-1}} \left( \gamma r_{a,i} \hat{y}_j^{(L-1)} \right) \\
 &= \sum_{j=1}^{n_{L-1}} W_{ij}^{(L)} y_j^{(L-1)} + \gamma r_{a,i} \sum_{j=1}^{n_{L-1}} \hat{y}_j^{(L-1)} \\
 &= y_i^{(L)} + \alpha r_i,
 \end{aligned}$$

which implies that  $\hat{y}^{(L)} = y^{(L)} + \gamma \alpha r_a = y^{(L)} + \alpha r$ .  $\square$

## B. Security Analysis of The Raw Training Data of Clients

In this section, we give a detailed analysis about the privacy-preservation of clients. Specifically, we first analyze how the traditional FL keeps the raw training data of clients from leaking to the server. Then, we prove that our PBPFL provides clients with the same level of privacy protection as the traditional FL.

### B.1. Privacy-preservation of The Raw Training Data in The Traditional FL

In the traditional FL, after local training, each client  $k$  ( $k \in \{1, 2, \dots, K\}$ ) returns the local gradients  $\{\frac{\partial \mathcal{L}}{\partial W_{ij}^{(l)}}\}_{l=1}^L$  to the server, where  $\frac{\partial \mathcal{L}}{\partial W_{ij}^{(l)}} = \frac{1}{|\mathcal{D}_k^t|} \sum_{n \in \mathcal{D}_k^t} \frac{\partial \mathcal{L}_n}{\partial W_{ij}^{(l)}}$  for  $i = 1, 2, \dots, n_l$  and  $j = 1, 2, \dots, n_{l-1}$ . Without loss of generality, we give the detailed calculation of one data  $(x_n, \bar{y}_n) \in \mathcal{D}_k^t$  as follows.

For  $l = 1, 2, \dots, L$ , the output vector  $y_n^{(l)}$  is a vector-valued function of  $y_n^{(l-1)}$ , then its Jacobian matrix denoted by  $W_n'^{(l)}$  can be computed as

$$W_n'^{(l)} = \begin{pmatrix} \frac{\partial y_{1,n}^{(l)}}{\partial y_{1,n}^{(l-1)}} & \frac{\partial y_{1,n}^{(l)}}{\partial y_{2,n}^{(l-1)}} & \cdots & \frac{\partial y_{1,n}^{(l)}}{\partial y_{n_{l-1},n}^{(l-1)}} \\ \frac{\partial y_{2,n}^{(l)}}{\partial y_{1,n}^{(l-1)}} & \frac{\partial y_{2,n}^{(l)}}{\partial y_{2,n}^{(l-1)}} & \cdots & \frac{\partial y_{2,n}^{(l)}}{\partial y_{n_{l-1},n}^{(l-1)}} \\ \vdots & \vdots & \ddots & \vdots \\ \frac{\partial y_{n_{l-1},n}^{(l)}}{\partial y_{1,n}^{(l-1)}} & \frac{\partial y_{n_{l-1},n}^{(l)}}{\partial y_{2,n}^{(l-1)}} & \cdots & \frac{\partial y_{n_{l-1},n}^{(l)}}{\partial y_{n_{l-1},n}^{(l-1)}} \end{pmatrix} = \begin{pmatrix} W_{11,n}'^{(l)} & W_{12,n}'^{(l)} & \cdots & W_{1n_{l-1},n}'^{(l)} \\ W_{21,n}'^{(l)} & W_{22,n}'^{(l)} & \cdots & W_{2n_{l-1},n}'^{(l)} \\ \vdots & \vdots & \ddots & \vdots \\ W_{n_{l-1}1,n}'^{(l)} & W_{n_{l-1}2,n}'^{(l)} & \cdots & W_{n_{l-1}n_{l-1},n}'^{(l)} \end{pmatrix},$$

where based on the ReLU non-linear activation,  $W_{ij,n}'^{(l)}$  (for  $i = 1, 2, \dots, n_l$  and  $j = 1, 2, \dots, n_{l-1}$ ) satisfies that

$$W_{ij,n}'^{(l)} = \begin{cases} W_{ij}^{(l)}, & \text{if } y_{i,n}^{(l)} \neq 0, \\ 0, & \text{if } y_{i,n}^{(l)} = 0. \end{cases}$$

Then we have

$$\begin{aligned}
 \frac{\partial \mathcal{L}_n}{\partial W_{ij}^{(l)}} &= \frac{\partial \mathcal{L}_n}{\partial y_n^{(L)}} \frac{\partial y_n^{(L)}}{\partial y_n^{(L-1)}} \cdots \frac{\partial y_n^{(l+2)}}{\partial y_n^{(l+1)}} \frac{\partial y_n^{(l+1)}}{\partial y_n^{(l)}} \frac{\partial y_n^{(l)}}{\partial W_{ij}^{(l)}} \\
 &= \frac{\partial \mathcal{L}_n}{\partial y_n^{(L)}} \frac{\partial y_n^{(L)}}{\partial y_n^{(L-1)}} \cdots \frac{\partial y_n^{(l+2)}}{\partial y_n^{(l+1)}} \frac{\partial y_n^{(l+1)}}{\partial y_{i,n}^{(l)}} \frac{\partial y_{i,n}^{(l)}}{\partial W_{ij}^{(l)}} \\
 &= (y_n^{(L)} - \bar{y}_n)^T W_n'^{(L)} \cdots W_n'^{(l+2)} W_{i,n}'^{(l+1)} \frac{\partial y_{i,n}^{(l)}}{\partial W_{ij}^{(l)}} \\
 &= (y_n^{(L)} - \bar{y}_n)^T A_{i,n}^{(l)} \frac{\partial y_{i,n}^{(l)}}{\partial W_{ij}^{(l)}}, \tag{21}
 \end{aligned}$$

where  $A_{i,n}^{(l)} = W_n'^{(L)} \cdots W_n'^{(l+2)} W_{i,n}'^{(l+1)} \in \mathbb{R}^{n_L \times 1}$  and  $W_{i,n}'^{(l+1)} = (W_{1i,n}'^{(l+1)}, W_{2i,n}'^{(l+1)}, \dots, W_{n_{l+1}i,n}'^{(l+1)})^T$  is the  $i$ -th column of  $W_n'^{(l+1)}$ . Based on the ReLU non-linear activation,  $\frac{\partial y_{i,n}^{(l)}}{\partial W_{ij}^{(l)}}$  satisfies

$$\frac{\partial \mathbf{y}_{i,n}^{(l)}}{\partial W_{ij}^{(l)}} = \begin{cases} \mathbf{y}_{j,n}^{(l-1)}, & \text{if } \mathbf{y}_{i,n}^{(l)} \neq 0, \\ 0, & \text{if } \mathbf{y}_{i,n}^{(l)} = 0. \end{cases}$$

Obviously, for different samples,  $W_n^{(l)}$  as well as  $A_{i,n}^{(l)}$  are different. Due to the effect of the ReLU non-linear activation, the server does not know  $W_n^{(l)}$ , let alone  $A_{i,n}^{(l)}$ . Besides, the terms  $\mathbf{y}_n^{(L)}$  and  $\frac{\partial \mathbf{y}_{i,n}^{(l)}}{\partial W_{ij}^{(l)}}$  are the linear combinations of feature vector  $\mathbf{x}_n$  with a series of ReLU activation. Specifically, we denote  $\mathbf{y}_n^{(L)} - \bar{\mathbf{y}}_n = F_n(\mathbf{x}_n)$  and  $\frac{\partial \mathbf{y}_{i,n}^{(l)}}{\partial W_{ij}^{(l)}} = H_{ij,n}^{(l)}(\mathbf{x}_n)$ , where the non-linear functions  $F_n(\cdot)$  and  $H_{ij,n}^{(l)}(\cdot)$  are also unknown to the server. Thus according to Eq. (21), the local gradients  $\frac{\partial \mathcal{L}}{\partial W_{ij}^{(l)}}$  can be deduced as

$$\frac{\partial \mathcal{L}}{\partial W_{ij}^{(l)}} = \frac{1}{|\mathcal{D}_k^t|} \sum_{n \in \mathcal{D}_k^t} \frac{\partial \mathcal{L}_n}{\partial W_{ij}^{(l)}} = \frac{1}{|\mathcal{D}_k^t|} \sum_{n \in \mathcal{D}_k^t} F_n(\mathbf{x}_n) A_{i,n}^{(l)} H_{ij,n}^{(l)}(\mathbf{x}_n).$$

Without knowing the non-linear functions  $F_n(\cdot)$  and  $H_{ij,n}^{(l)}(\cdot)$  as well as the vector  $A_{i,n}^{(l)} \in \mathbb{R}^{n_L \times 1}$ , it is difficult for the server to resolve the training dataset  $\mathcal{D}_k^t$  of the  $k$ -th client from  $\frac{\partial \mathcal{L}}{\partial W_{ij}^{(l)}}$ , let alone each sample  $(\mathbf{x}_n, \bar{\mathbf{y}}_n) \in \mathcal{D}_k^t$ . Thus, it is generally believed that the traditional FL can provide the privacy-preservation for distributed clients to some extent.

## B.2. Privacy-preservation of The Raw Data in Our PBPFL

In our PBPFL scheme, in addition to the noisy local gradients, each client  $k$  has to return two additional noisy terms  $\{\boldsymbol{\sigma}^{(l)}, \boldsymbol{\beta}^{(l)}\}_{l=1}^L$  to the server for recovering the true gradients. Thus, the key is to prove the difficulty of obtaining  $(\mathbf{x}_n, \bar{\mathbf{y}}_n)$  from  $\{\boldsymbol{\sigma}^{(l)}, \boldsymbol{\beta}^{(l)}\}_{l=1}^L$ .

As shown in Lemma 2 in Section 3.2,  $\boldsymbol{\sigma}_{ij}^{(l)}$  and  $\boldsymbol{\beta}_{ij}^{(l)}$  are computed as

$$\begin{cases} \boldsymbol{\sigma}_{ij}^{(l)} = \frac{1}{|\mathcal{D}_k^t|} \sum_{n \in \mathcal{D}_k^t} \boldsymbol{\sigma}_{ij,n}^{(l)} = \frac{1}{|\mathcal{D}_k^t|} \sum_{n \in \mathcal{D}_k^t} \mathbf{r}_a^T \left( \alpha_n \frac{\partial \hat{\mathbf{y}}_n^{(L)}}{\partial \widehat{W}_{ij}^{(l)}} + \frac{\partial \alpha_n}{\partial \widehat{W}_{ij}^{(l)}} \left( \frac{\partial \mathcal{L}_n}{\partial \hat{\mathbf{y}}_n^{(L)}} \right)^T \right) \\ \boldsymbol{\beta}_{ij}^{(l)} = \frac{1}{|\mathcal{D}_k^t|} \sum_{n \in \mathcal{D}_k^t} \boldsymbol{\beta}_{ij,n}^{(l)} = \frac{1}{|\mathcal{D}_k^t|} \sum_{n \in \mathcal{D}_k^t} \alpha_n \frac{\partial \alpha_n}{\partial \widehat{W}_{ij}^{(l)}}. \end{cases} \quad (22)$$

Similar to Section B.1, we give the details of  $\boldsymbol{\sigma}_{ij,n}^{(l)}$  and  $\boldsymbol{\beta}_{ij,n}^{(l)}$ . More specifically, the noisy Jacobian matrix  $\widehat{W}_n^{(l)}$  of the noisy output vector  $\hat{\mathbf{y}}_n^{(l)}$  is computed as

$$\widehat{W}_n^{(l)} = \begin{pmatrix} \frac{\partial \hat{y}_{1,n}^{(l)}}{\partial \hat{y}_{1,n}^{(l-1)}} & \frac{\partial \hat{y}_{1,n}^{(l)}}{\partial \hat{y}_{2,n}^{(l-1)}} & \cdots & \frac{\partial \hat{y}_{1,n}^{(l)}}{\partial \hat{y}_{n_l-1,n}^{(l-1)}} \\ \frac{\partial \hat{y}_{2,n}^{(l)}}{\partial \hat{y}_{1,n}^{(l-1)}} & \frac{\partial \hat{y}_{2,n}^{(l)}}{\partial \hat{y}_{2,n}^{(l-1)}} & \cdots & \frac{\partial \hat{y}_{2,n}^{(l)}}{\partial \hat{y}_{n_l-1,n}^{(l-1)}} \\ \vdots & \vdots & \ddots & \vdots \\ \frac{\partial \hat{y}_{n_l,n}^{(l)}}{\partial \hat{y}_{1,n}^{(l-1)}} & \frac{\partial \hat{y}_{n_l,n}^{(l)}}{\partial \hat{y}_{2,n}^{(l-1)}} & \cdots & \frac{\partial \hat{y}_{n_l,n}^{(l)}}{\partial \hat{y}_{n_l-1,n}^{(l-1)}} \end{pmatrix} = \begin{pmatrix} \widehat{W}_{11,n}^{(l)} & \widehat{W}_{12,n}^{(l)} & \cdots & \widehat{W}_{1n_l-1,n}^{(l)} \\ \widehat{W}_{21,n}^{(l)} & \widehat{W}_{22,n}^{(l)} & \cdots & \widehat{W}_{2n_l-1,n}^{(l)} \\ \vdots & \vdots & \ddots & \vdots \\ \widehat{W}_{n_l1,n}^{(l)} & \widehat{W}_{n_l2,n}^{(l)} & \cdots & \widehat{W}_{n_ln_l-1,n}^{(l)} \end{pmatrix},$$

where

$$\widehat{W}_{ij,n}^{(l)} = \begin{cases} \widehat{W}_{ij}^{(l)}, & \text{if } \hat{\mathbf{y}}_{i,n}^{(l)} \neq 0, \\ 0, & \text{if } \hat{\mathbf{y}}_{i,n}^{(l)} = 0. \end{cases}$$

Similar to Eq. (21), we have

$$\frac{\partial \hat{\mathbf{y}}_n^{(L)}}{\partial \widehat{W}_{ij}^{(l)}} = \widehat{W}_n^{(L)} \cdots \widehat{W}_n^{(l+2)} \widehat{W}_{i,n}^{(l+1)} \frac{\partial \hat{\mathbf{y}}_{i,n}^{(l)}}{\partial \widehat{W}_{ij}^{(l)}},$$

where  $\widehat{W}_{i,n}^{(l+1)} = (\widehat{W}_{1,i,n}^{(l+1)}, \widehat{W}_{2,i,n}^{(l+1)}, \dots, \widehat{W}_{n_{l+1},i,n}^{(l+1)})^T$  is the  $i$ -th column of  $\widehat{W}_n^{(l+1)}$  and

$$\frac{\partial \widehat{\mathbf{g}}_{i,n}^{(l)}}{\partial \widehat{W}_{ij}^{(l)}} = \begin{cases} \widehat{\mathbf{g}}_{j,n}^{(l-1)}, & \text{if } \widehat{\mathbf{g}}_{i,n}^{(l)} \neq 0, \\ 0, & \text{if } \widehat{\mathbf{g}}_{i,n}^{(l)} = 0. \end{cases}$$

Moreover,  $\frac{\partial \alpha_n}{\partial \widehat{W}_{ij}^{(l)}}$  is computed as

$$\frac{\partial \alpha_n}{\partial \widehat{W}_{ij}^{(l)}} = \frac{\partial \alpha_n}{\partial \widehat{\mathbf{g}}_n^{(L-1)}} \frac{\partial \widehat{\mathbf{g}}_n^{(L-1)}}{\partial \widehat{W}_{ij}^{(l)}} = e \widehat{W}_n^{(L-1)} \dots \widehat{W}_n^{(l+2)} \widehat{W}_{i,n}^{(l+1)} \frac{\partial \widehat{\mathbf{g}}_{i,n}^{(l)}}{\partial \widehat{W}_{ij}^{(l)}},$$

where  $e = (1, 1, \dots, 1)_{1 \times n_{L-1}}$ .

Similarly, let  $\widehat{A}_{i,n}^{(l)} = \widehat{W}_n^{(L)} \dots \widehat{W}_n^{(l+2)} \widehat{W}_{i,n}^{(l+1)} \in \mathbb{R}^{n_L \times 1}$ ,  $\widehat{B}_{i,n}^{(l)} = \widehat{W}_n^{(L-1)} \dots \widehat{W}_n^{(l+2)} \widehat{W}_{i,n}^{(l+1)} \in \mathbb{R}^{n_{L-1} \times 1}$  and  $\frac{\partial \widehat{\mathbf{g}}_{i,n}^{(l)}}{\partial \widehat{W}_{ij}^{(l)}} = \widehat{H}_{ij,n}^{(l)}(\mathbf{x}_n)$ . Note that  $\alpha_n = \sum_{i=1}^{n_{L-1}} \widehat{\mathbf{g}}_{i,n}^{(L-1)}$ , which is also a non-linear function of  $\mathbf{x}_n$  and denoted as  $\alpha_n = \sum_{i=1}^{n_{L-1}} \widehat{F}_{i,n}^{(L-1)}(\mathbf{x}_n)$ . Thus, from Eq. (22), we have

$$\begin{aligned} \sigma_{ij}^{(l)} &= \frac{1}{|\mathcal{D}_k^t|} \sum_{n \in \mathcal{D}_k^t} \mathbf{r}_a^T \left( \alpha_n \frac{\partial \widehat{\mathbf{g}}_n^{(L)}}{\partial \widehat{W}_{ij}^{(l)}} + \frac{\partial \alpha_n}{\partial \widehat{W}_{ij}^{(l)}} \left( \frac{\partial \widehat{\mathcal{L}}_n}{\partial \widehat{\mathbf{g}}_n^{(L)}} \right)^T \right) \\ &= \frac{1}{|\mathcal{D}_k^t|} \mathbf{r}_a^T \sum_{n \in \mathcal{D}_k^t} \left( \left( \sum_{i=1}^{n_{L-1}} \widehat{F}_{i,n}^{(L-1)}(\mathbf{x}_n) \right) \widehat{A}_{i,n}^{(l)} \widehat{H}_{ij,n}^{(l)}(\mathbf{x}_n) + e \widehat{B}_{i,n}^{(l)} \widehat{H}_{ij,n}^{(l)}(\mathbf{x}_n) \right) \\ &= \frac{1}{|\mathcal{D}_k^t|} \mathbf{r}_a^T \sum_{n \in \mathcal{D}_k^t} \widehat{H}_{ij,n}^{(l)}(\mathbf{x}_n) \left( \left( \sum_{i=1}^{n_{L-1}} \widehat{F}_{i,n}^{(L-1)}(\mathbf{x}_n) \right) \widehat{A}_{i,n}^{(l)} + e \widehat{B}_{i,n}^{(l)} \right) \end{aligned}$$

and

$$\beta_{ij}^{(l)} = \frac{1}{|\mathcal{D}_k^t|} \sum_{n \in \mathcal{D}_k^t} \alpha_n \frac{\partial \alpha_n}{\partial \widehat{W}_{ij}^{(l)}} = \frac{1}{|\mathcal{D}_k^t|} e \sum_{n \in \mathcal{D}_k^t} \left( \sum_{i=1}^{n_{L-1}} \widehat{F}_{i,n}^{(L-1)}(\mathbf{x}_n) \right) \widehat{H}_{ij,n}^{(l)}(\mathbf{x}_n) \widehat{B}_{i,n}^{(l)}.$$

From the above, we can see that without knowing  $\widehat{A}_{i,n}^{(l)} \in \mathbb{R}^{n_L \times 1}$ ,  $\widehat{B}_{i,n}^{(l)} \in \mathbb{R}^{n_{L-1} \times 1}$ ,  $\widehat{H}_{ij,n}^{(l)}(\cdot)$  and  $\widehat{F}_{i,n}^{(L-1)}(\cdot)$ , resolving each sample  $(\mathbf{x}_n, \bar{\mathbf{y}}_n) \in \mathcal{D}_k^t$  from additional noisy terms  $\sigma_{ij}^{(l)}$  and  $\beta_{ij}^{(l)}$  is as difficult as resolving from the gradients.

Thus, we can obtain that the level of privacy protection of the raw training data of clients in our PBPFL is the same as the traditional FL. Actually, our PBPFL can further improve the privacy-preservation for clients by adopting the secret sharing technique. In what follows, we give more details about this improvement.

## C. Further Enhancement of The PBPFL

In this section, we present an enhancement of our PBPFL that improves the privacy-preservation of the local training data by preventing the honest-but-curious server from obtaining individual noisy local gradients as well as the corresponding noisy terms. Our approach is to extend the PBPFL so that all clients cooperate in selecting a group of random numbers that will be added to the results of noisy gradient computation.

### C.1. The Extended PBPFL

The extended PBPFL can guarantee that the honest-but-curious server can only recover the aggregated gradients for all clients rather than individual local gradients. Specifically, the parameter perturbation and noisy gradient computation are as described in Sections 3.1 and 3.2. We only add the secret sharing technique after noisy gradient computation and modify the operation of gradient recovery in Section 3.3 as follows.

**(1) Noisy local gradients perturbation.** All  $K$  clients consult with a set of random number matrices  $\{\boldsymbol{\lambda}_1^{(l)}, \boldsymbol{\lambda}_2^{(l)}, \dots, \boldsymbol{\lambda}_K^{(l)}\}$  such that  $\sum_{k=1}^K N_k \boldsymbol{\lambda}_k^{(l)} = \mathbf{0}_{n_l \times n_{l-1}}$  for  $l = 1, 2, \dots, L$ , which are unknown to the server. Without loss of generality, we

assume the  $k$ -th client holds  $\{\lambda_k^{(l)}\}_{l=1}^L$ . Note that for different iteration, clients can consult with different a set of random number matrices. After each client  $k$  computes the noisy local gradients  $\left\{\left(\frac{\partial \hat{\mathcal{L}}}{\partial \widehat{W}^{(l)}}\right)_k\right\}_{l=1}^L$  as well as two noisy terms  $\{\sigma_k^{(l)}, \beta_k^{(l)}\}_{l=1}^L$ , the  $k$ -th client masks them with the secret parameter  $\lambda_k^{(l)}$  as follows:

$$\nabla \widehat{F}_k(\widehat{W}^{(l)}) = \left(\frac{\partial \hat{\mathcal{L}}}{\partial \widehat{W}^{(l)}}\right)_k + \lambda_k^{(l)} \quad (23)$$

$$\widehat{\sigma}_k^{(l)} = \sigma_k^{(l)} + \lambda_k^{(l)} \quad (24)$$

$$\widehat{\beta}_k^{(l)} = \beta_k^{(l)} + \lambda_k^{(l)} \quad (25)$$

Note that  $\lambda_k^{(l)}$  in Eqs. (23), (24) and (25) can be different, for simplicity, we do not use other symbols to distinguish. Then, the  $k$ -th client returns  $\{\nabla \widehat{F}_k(\widehat{W}^{(l)})\}_{l=1}^L$  together with two noisy terms  $\{\widehat{\sigma}_k^{(l)}, \widehat{\beta}_k^{(l)}\}_{l=1}^L$  to the server.

**(1) Model update.** Compared to Section 3.3 in the basic PBPFL, in the extended PBPFL, the server first needs to aggregate received data from all clients, and then recover the exact aggregated gradients. More specifically, the server computes

$$\nabla \widehat{F}(\widehat{W}^{(l)}) = \sum_{k=1}^K \frac{N_k}{N} \nabla \widehat{F}_k(\widehat{W}^{(l)}) = \sum_{k=1}^K \frac{N_k}{N} \left( \frac{\partial \hat{\mathcal{L}}}{\partial \widehat{W}^{(l)}} + \lambda_k^{(l)} \right) = \sum_{k=1}^K \frac{N_k}{N} \frac{\partial \hat{\mathcal{L}}}{\partial \widehat{W}^{(l)}} + \mathbf{0}_{n_l \times n_{l-1}} = \sum_{k=1}^K \frac{N_k}{N} \frac{\partial \hat{\mathcal{L}}}{\partial \widehat{W}^{(l)}}, \quad (26)$$

$$\widehat{\sigma}^{(l)} = \sum_{k=1}^K \frac{N_k}{N} \widehat{\sigma}_k^{(l)} = \sum_{k=1}^K \frac{N_k}{N} (\sigma_k^{(l)} + \lambda_k^{(l)}) = \sum_{k=1}^K \frac{N_k}{N} \sigma_k^{(l)} + \mathbf{0}_{n_l \times n_{l-1}} = \sum_{k=1}^K \frac{N_k}{N} \sigma_k^{(l)}, \quad (27)$$

$$\widehat{\beta}^{(l)} = \sum_{k=1}^K \frac{N_k}{N} \widehat{\beta}_k^{(l)} = \sum_{k=1}^K \frac{N_k}{N} (\beta_k^{(l)} + \lambda_k^{(l)}) = \sum_{k=1}^K \frac{N_k}{N} \beta_k^{(l)} + \mathbf{0}_{n_l \times n_{l-1}} = \sum_{k=1}^K \frac{N_k}{N} \beta_k^{(l)}, \quad (28)$$

where  $l = 1, 2, \dots, L$ .

Then, according to Lemma 2, the server recovers the true aggregated gradients  $\nabla F(W^{(l)})$  as follows:

$$\begin{aligned} \nabla F(W^{(l)}) &= R^{(l)} \circ \left( \nabla \widehat{F}(\widehat{W}^{(l)}) - \gamma \widehat{\sigma}^{(l)} + v \widehat{\beta}^{(l)} \right) \\ &= R^{(l)} \circ \left( \sum_{k=1}^K \frac{N_k}{N} \frac{\partial \hat{\mathcal{L}}}{\partial \widehat{W}^{(l)}} - \gamma \sum_{k=1}^K \frac{N_k}{N} \sigma_k^{(l)} + v \sum_{k=1}^K \frac{N_k}{N} \beta_k^{(l)} \right) \\ &= R^{(l)} \circ \left( \sum_{k=1}^K \frac{N_k}{N} \left( \frac{1}{R^{(l)}} \circ \frac{\partial \mathcal{L}}{\partial W^{(l)}} + \gamma \sigma_k^{(l)} - v \beta_k^{(l)} \right) - \gamma \sum_{k=1}^K \frac{N_k}{N} \sigma_k^{(l)} + v \sum_{k=1}^K \frac{N_k}{N} \beta_k^{(l)} \right) \\ &= R^{(l)} \circ \left( \sum_{k=1}^K \frac{N_k}{N} \frac{1}{R^{(l)}} \circ \frac{\partial \mathcal{L}}{\partial W^{(l)}} + \sum_{k=1}^K \frac{N_k}{N} \gamma \sigma_k^{(l)} - \sum_{k=1}^K \frac{N_k}{N} v \beta_k^{(l)} - \gamma \sum_{k=1}^K \frac{N_k}{N} \sigma_k^{(l)} + v \sum_{k=1}^K \frac{N_k}{N} \beta_k^{(l)} \right) \\ &= R^{(l)} \circ \sum_{k=1}^K \frac{N_k}{N} \frac{1}{R^{(l)}} \circ \frac{\partial \mathcal{L}}{\partial W^{(l)}} \\ &= R^{(l)} \circ \frac{1}{R^{(l)}} \circ \sum_{k=1}^K \frac{N_k}{N} \frac{\partial \mathcal{L}}{\partial W^{(l)}} \\ &= \sum_{k=1}^K \frac{N_k}{N} \frac{\partial \mathcal{L}}{\partial W^{(l)}}. \end{aligned} \quad (30)$$

Note that Eq. (30) holds when the multiplicative noisy vectors  $\{r^{(l)}\}_{l=1}^L$ , the additive noisy vector  $r_a$  and a random coefficient  $\gamma$  for all clients are the same. In other words, the noisy parameters  $\{\widehat{W}^{(l)}\}_{l=1}^L$  sent to all clients are the same.

Finally, the server updates the global model parameters for the  $(t+1)$ -th iteration as

$$W_{t+1}^{(l)} \leftarrow W^{(l)} - \eta \nabla F(W^{(l)}), \text{ for } l = 1, 2, \dots, L$$

where  $W^{(l)}$  is the parameters of the current iteration, i.e., the  $t$ -th iteration.



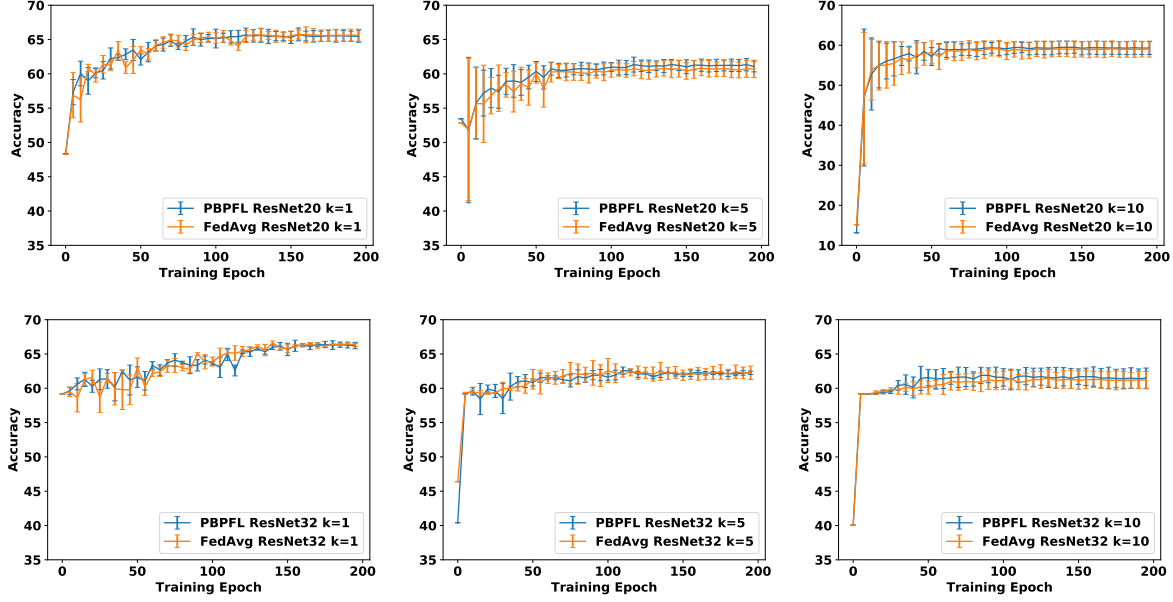


Figure 3. Training curves for PBPFL and FedAvg. The first and second rows demonstrate the results for ResNet20 and ResNet32 with 1, 5 and 10 clients respectively. The error bars stand for standard deviation and are shown every 5 epochs. Each experiment is repeated 5 times. Please note that it is best to view in color.

## C.2. Security Analysis

In this section, we mainly analyze the privacy-preserving of the raw training data. Since the server does not know the random number matrices  $\{\lambda_1^{(l)}, \lambda_2^{(l)}, \dots, \lambda_K^{(l)}\}_{l=1}^L$ , given  $\nabla \hat{F}_k(\widehat{W}^{(l)})$ , there exist infinite pairs  $\left(\left(\frac{\partial \hat{\mathcal{L}}}{\partial \widehat{W}^{(l)}}\right)_k, \lambda_k^{(l)}\right)$  satisfy Eq. (23). Therefore, the server cannot identify the noisy gradients  $\left(\frac{\partial \hat{\mathcal{L}}}{\partial \widehat{W}^{(l)}}\right)_k$  of the  $k$ -th client. Similarly, the server also cannot identify individual additional noisy terms  $\{\sigma_k^{(l)}, \beta_k^{(l)}\}$ . Consequently, it is almost impossible for the server to obtain the true gradients of each client, let alone the local training data. Note that in the cross-silo FL (Kairouz et al., 2019), clients are different organizations (e.g. medical or financial), the network connection is relatively stable and the network bandwidth is relatively large. Thus, we can neglect the stragglers that cannot return the model updates to the server. That is, all clients can return model updates in time.

## D. Additional Experiment Results

The main purpose of our PBPFL is to enable clients to train over noisy models without accuracy loss. In this section, we further empirically prove this claim by comparing the training curve of our PBPFL against one of the most popular traditional FL aggregation algorithms, i.e., FedAvg (McMahan et al., 2017).

We train ResNet20 and ResNet32 (He et al., 2016) models on Lesion Disease Classification dataset (Tschandl et al., 2018) (Codella et al., 2019) for 200 epochs for PBPFL and FedAvg, respectively. For the fairness of comparison, we use different random seeds for each run, and set the seeds for PBPFL and FedAvg to be the same. Then we demonstrate the mean and standard deviation of test accuracy after each epoch in Figure 3. As shown in the figure, overall, the training curve of PBPFL and FedAvg aligns well. Although the PBPFL curve and the FedAvg curve may be noisy in the early stage, they tend to stabilize and converge to similar results as the training proceeds.